European Journal of Pharmaceutics and Biopharmaceutics 74 (2010) 474–482

Contents lists available at ScienceDirect

European Journal of Pharmaceutics and Biopharmaceutics

journal homepage: www.elsevier.com/locate/ejpb

Research paper

Effects of lipophilic emulsifiers on the oral administration of lovastatin from nanostructured lipid carriers: Physicochemical characterization and pharmacokinetics

Chih-Chieh Chen [a], Tung-Hu Tsai [b,c], Zih-Rou Huang [a], Jia-You Fang [a,d,*]

[a] Pharmaceutics Laboratory, Graduate Institute of Natural Products, Chang Gung University, Taoyuan, Taiwan
[b] Institute of Traditional Medicine, School of Medicine, National Yang-Ming University, Taipei, Taiwan
[c] Department of Education and Research, Taipei City Hospital, Taipei, Taiwan
[d] Department of Pharmaceutics, College of Pharmacy, King Saud University, Riyadh, Saudi Arabia

ARTICLE INFO

Article history:
Received 9 October 2009
Accepted in revised form 21 December 2009
Available online 7 January 2010

Keywords:
Lovastatin
Lipid nanoparticles
Nanostructured lipid carriers
Oral administration
Emulsifier
Pharmacokinetics

ABSTRACT

Nanostructured lipid carriers (NLCs) made from mixtures of Precirol and squalene were prepared to investigate whether the bioavailability of lovastatin can be improved by oral delivery. The size, zeta potential, drug-loading capacity, and release properties of the NLCs were compared with those of lipid nanoparticles containing pure Precirol (solid lipid nanoparticles, SLNs) and squalene (lipid emulsions, LEs). Stable nanoparticles with a mean size range of 180–290 nm and zeta potential range of −3 to −35 mV were developed. More than 70% lovastatin was entrapped in the NLCs and LEs, which was significantly higher compared to the SLNs. The in vitro release kinetics demonstrated that lovastatin release could be reduced by up to 60% with lipid nanoparticles containing Myverol as the lipophilic emulsifier, which showed a decreasing order of NLCs > LEs > SLNs. Drug release was further decreased by soybean phosphatidylcholine (SPC) incorporation, with NLCs and SLNs showing the slowest delivery. The oral lovastatin bioavailability was enhanced from 4% to 24% and 13% when the drug was administered from NLCs containing Myverol and SPC, respectively. The in vivo real-time bioluminescence imaging indicated superior stability of the Myverol system over the SPC system in the gastric environment.

1. Introduction

Several approaches have been investigated to develop nano-sized drug delivery systems in recent years. These systems can generally be divided into two groups: polymeric and lipidic systems [1]. The number of products based on polymeric nanoparticles in the market is limited because of the toxicity of polymers and the lack of suitable large-scale production methods. In order to overcome these problems, a great deal of interest has focused on lipid-based carriers such as solid lipid nanoparticles (SLNs) and lipid emulsions (LEs). SLNs and LEs are colloidal systems prepared from solid and liquid lipids, respectively. These systems have advantages for drug delivery, such as the use of physiologically tolerated lipids, large-scale production, protection of drugs from degradation, improved bioavailability, and controlled-release characteristics [2]. Common disadvantages of SLNs include limited drug loading capacities and drug expulsion during storage [3]. Moreover, one of the reasons preventing a broad introduction of LEs is their physical instability which can be exacerbated by the incorporated drug [4]. Nanostructured lipid carriers (NLCs) composed of a solid lipid matrix with a certain content of a liquid lipid are a new generation of lipid nanoparticles. NLCs are considered a smarter generation of nanoparticles which possess improved properties for drug loading, modulation of the delivery profile, and stable drug incorporation during storage [5]. Due to the lipophilic nature of the matrix produced, NLCs are considered particularly useful for the administration of lipophilic drugs.

Lovastatin, a cholesterol-lowering agent isolated from a strain of *Aspergillus terreus*, is a highly effective and generally well-tolerated treatment for patients with moderate hypercholesterolemia [6]. It is a prodrug and is converted by esterases from its lactone to the active and open acidic form. Lovastatin also exhibits pharmacological activities of bone formation and chemoprevention [7,8]. Lovastatin exhibits poor oral bioavailability of <5% because of rapid metabolism in the gut and liver [9]. Lovastatin and its active β-hydroxyacid metabolite have short half-lives (1–2 h), and steady-state concentrations are achieved within 2–3 days [10]. A formulation with a high degree of oral absorption and extended delivery potential would be highly desirable for lovastatin.

* Corresponding author. Address: Pharmaceutics Laboratory, Graduate Institute of Natural Products, Chang Gung University, 259 Wen-Hwa 1st Road, Kweishan, Taoyuan 333, Taiwan. Tel.: +886 3 2118800x5521; fax: +886 3 2118236.
E-mail address: fajy@mail.cgu.edu.tw (J.-Y. Fang).

0939-6411/$ - see front matter © 2010 Elsevier B.V. All rights reserved.
doi:10.1016/j.ejpb.2009.12.008

The aim of the present work was to load lovastatin as a model drug into NLCs with enhanced oral absorption and controlled release properties. Precirol and squalene were chosen as the solid and liquid lipids, respectively. If the obtained blood profile after oral ingestion is not optimal, it can be modulated by changing the composition of the nanoparticles, mainly the emulsifiers [11]. A variety of different emulsifiers have been used to prepare NLCs, including Pluronic F68 (PF68), Myverol 18–04 K, and soybean phosphatidylcholine (SPC). Nanoparticles with different Precirol/squalene ratios were prepared in this study and characterized by the size, zeta potential, drug encapsulation ratio, polarity in a molecular environment, and drug release behavior. The in vivo pharmacokinetics of lovastatin-loaded NLCs were evaluated to elucidate their feasibility as oral delivery systems. The bioluminescence imaging modality was used to monitor the distribution of NLCs in the gastrointestinal (GI) tract.

2. Materials and methods

2.1. Materials

Lovastatin with a purity of 99.13% was kindly provided by Syngen Biotech (Tainan, Taiwan). Squalene, Pluronic F68 (PF68), Nile red, Sephadex G-15, Triton X-100, and sulforhodamine B were purchased from Sigma–Aldrich Chemical (St. Louis, MO, USA). Precirol ATO 5 was supplied by Gattefossé (Gennevilliers, France). Myverol 18–04 K was obtained from Quest (Naarden, The Netherlands). Hydrogenated soybean phosphatidylcholine (SPC, Phospholipon 80H®) was from American Lecithin (Oxford, CT, USA).

2.2. Preparation of lipid nanoparticles

The lipid and aqueous phases were prepared separately. The solid lipid/liquid lipid phase consisted of 10% (w/v) Precirol and squalene at different ratios and 0.2% Myverol or SPC as the lipophilic emulsifier, while the aqueous phase consisted of double-distilled water (ddH_2O) and a hydrophilic emulsifier (2.8% PF68). Lovastatin (1%) was positioned in the lipid phase. Both phases were heated separately to 85 °C for 10 min. The aqueous phase was added to the lipid phase and mixed using a high-shear homogenizer (Pro 250, Pro Scientific, Monroe, CT, USA) at 12,000 rpm for 10 min. The mixture was further treated using a probe-type sonicator (VCX600, Sonics and Materials, Newtown, CT, USA) for 10 min at 35 W. The lipid phases consisting of 100% Precirol, 100% squalene, and the Precirol/squalene mixture were denoted the SLNs, LEs, and NLCs, respectively.

2.3. Particle size and zeta potential measurements

The mean particle size (*z*-average) of the nanoparticles was measured by photon correlation spectroscopy (Nano ZS90, Malvern, Worcestershire, UK) at 25 °C and a 90° scattering angle. The zeta potential determination was based on the particle electrophoretic mobility in aqueous medium. A 1:100 dilution of the systems was made using ddH_2O before the measurements.

2.4. Drug encapsulation efficiency

Unencapsulated lovastatin was removed by size exclusion chromatography on a Sephadex G-15 column using ddH_2O as the eluent. The encapsulation efficiency was determined by dissolving 0.5 ml of the lipid nanoparticles obtained from gel chromatography in 0.5 ml of Triton X-100 (1%) and diluting this with ddH_2O (100×), followed by measurement by high-performance liquid chromatography (HPLC). The HPLC analytical method for lovastatin was described previously [12]. In brief, the HPLC system included an L7100 pump, an L7200 sample processor, and an L7400 UV detector all from Hitachi (Tokyo, Japan). A Merck LiChrosorb RP18 column (250 × 4 mm i.d.; particle size 5 μm) was used as the stationary phase. The mobile phase was an acetonitrile: 10 mM NaH_2PO_4 (60:40) mixture at a flow rate of 1 ml/min. The UV detection wavelength was 237 nm. The encapsulation percentage (%) was determined by the following equation:

$$\text{Encapsulation percentage } (\%) = W_E/W_A \times 100\%,$$

where W_E is the amount of lovastatin in the nanoparticles, and W_A is the amount of lovastatin in the system.

2.5. Molecular environment of lipid nanoparticles

The lipophilic fluorescent marker, Nile red, was used as the model solute, and the molecular environment (polarity) was determined by fluorometric spectrophotometry based on the solvatochromism of Nile red. The lipid nanoparticles with 1 ppm Nile red were prepared as described above. Emission fluorescence spectra were determined with a Hitachi F-2500 spectrometer (Tokyo, Japan). The spectra of NLCs with Nile red were recorded with both slit widths set to 10 nm. The λ_{ex} was fixed at 546 nm, and the emission spectra were recorded from 570 to 700 nm at a scanning speed of 300 nm/min.

2.6. Partitioning of the drug between lipids and water

The partition coefficient was determined by equilibration of lovastatin partitioning between the melted lipid phase and water phase. Lovastatin (150 μg) was dispersed in a mixture of melted lipid (1 g) with various Precirol/squalene ratios and 1 ml of ddH_2O. The mixture was shaken reciprocally in a water bath at 85 °C for 30 min and then centrifuged at 5500 rpm for 10 min. The aqueous phase was filtered through a polyvinylidene difluoride (PVDF) membrane with a pore size of 0.45 μm. The drug concentrations in the lipids and water were determined by HPLC. Partitioning was calculated as log *P* (log (drug concentration in the lipid phase/drug concentration in the water phase)).

2.7. In vitro release kinetics of the drug from lipid nanoparticles

The drug released from the carriers was measured using a Franz diffusion cell. A cellulose membrane (Cellu-Sep® T2, with a molecular weight cutoff of 6000–8000) was mounted between the donor and receptor compartments. The donor medium consisted of 0.5 ml of vehicle containing lovastatin (1%). The receptor medium consisted of 5.5 ml of 30% ethanol in pH 7.4 buffer to maintain sink conditions. The available diffusion area between cells was 0.785 cm^2. The stirring rate and temperature were 600 rpm and 37 °C, respectively. At appropriate intervals, 300-μl aliquots of the receptor medium were withdrawn and immediately replaced with an equal volume of fresh buffer. The amount of drug released was determined by an HPLC method.

2.8. Animals

The in vivo experiments were performed on male Sprague–Dawley rats (200–230 g). The animal experiment protocol was reviewed and approved by the Institutional Animal Care and Use Committee of Chang Gung University. Animals were housed and handled according to institutional guidelines. The ethical issues with animal experiments complied with Directive 86/609/EEC from European Commission. All animals were starved overnight prior to the experiments.

2.9. In vivo pharmacokinetics

All rats were anesthetized with intraperitoneal pentobarbital (50 mg/kg). The body temperature of rats was maintained at 37 °C with a heating pad. Lovastatin was given orally (100 mg/kg), or the femoral vein was exposed for a lovastatin injection (10 mg/kg). Oral formulations were delivered by an oral intubation cannula. A parenteral solution was injected through the catheter. An aliquot of a 200-μl blood sample was withdrawn from a jugular vein into a heparin-rinsed vial according to a programmed schedule at 10, 30, 60, 90, 120, 180, and 240 min after dosing. Each blood sample was centrifuged at 3000*g* for 10 min. The resulting plasma sample (100 μl) was vortex-mixed with 150 μl of internal standard (chlorpromazine, 2.8 μg/ml) in acetonitrile. The denatured protein precipitate was separated by centrifugation at 8000*g* for 10 min. An aliquot (20 μl) of the supernatant was directly injected into HPLC for analysis. At the range 0.1–100 μg/ml, the concentration of lovastatin was linearly proportional to their chromatographic peak area/internal standard area (correlation value of >0.995). The limit of detection (LOD) of lovastatin was determined to be 25 ng/ml. The intra- and inter-assay precision and accuracy values were evaluated at the concentration range 0.1–100 μg/ml. The overall precision, defined by the relative standard deviation (RSD), ranged from 2.1% to 7.8% on average. Analytical accuracy, expressed as the percentage difference between the mean of measured value and the known concentration, varied from −5.8% to 7.7%.

2.10. Data analysis

Pharmacokinetic calculations were performed on each set of data using the pharmacokinetic software WinNonlin Standard Edition Version 1.1 (Pharsight, Mountain View, CA, USA) using a non-compartmental method. The maximum concentration, C_{max}, and the time to reach C_{max} (t_{max}) were determined by observing individual animal concentrations versus time curves. The area under the plasma concentration curve from the time of administration to infinity ($AUC_{0\to\infty}$) was calculated using the trapezoidal rule with extrapolation to infinity. The absolute bioavailability (F) of the oral formulations was estimated as the $AUC_{0\to\infty}$ ratio of the oral dosage form to the parenteral solution after dose calibration. The mean residence time (MRT) was estimated by $MRT = AUMC_{0\to\infty}/AUC_{0\to\infty}$. The elimination half-life ($t_{1/2}$) was calculated from the elimination rate constant (k_e) estimated by a linear-square regression on the final plasmatic concentrations of lovastatin. The volume of distribution (V_z/F) was calculated according to dose/$k_e \times AUC_{0\to\infty}$.

2.11. In vivo bioluminescence imaging

In vivo bioluminescence imaging was performed with an IVIS® 200 imaging system (Xenogen, Alameda, CA, USA) linked to Living Image® 3.1 software (Xenogen). This system provides high signal-to-noise images of fluorescence signals emerging from within living animals. Sulforhodamine B as the fluorescence dye was added to NLCs at a concentration of 0.92 mg/ml. A 1 ml/kg control solution (propylene glycol:ethanol = 9:1) or NLCs was given by oral gavage. Animals were placed prone in a light-tight chamber, where a controlled flow of 1.5% isoflurane in air was administered through a nose cone via a gas anesthesia system. A gray-scale reference image was obtained under low-level illumination. The images were monitored 10 min after oral administration. Optical excitation was carried out at 605 nm, and the emission wavelength was detected at 680 nm. All experimental results were repeated on at least three different animals, and representative pictures are shown.

2.12. Statistical analysis

The statistical analysis of differences among various treatments was performed using unpaired Student's t-test. A 0.05 level of probability was taken as the level of significance. An analysis of variance (ANOVA) test was also used if necessary.

3. Results

3.1. Particle size and zeta potential measurements

Lipid nanoparticles were produced by hot homogenization followed by ultrasonication. Precirol, a glyceryl palmito-stearate, was used as a solid matrix for the nanoparticles. Squalene as the liquid matrix was mixed with Precirol to form NLCs. Squalene is an all-trans-isoprenoid containing six isoprene units and is a naturally occurring substance found in humans. Nanoparticles with different Precirol/squalene ratios from 10:0 to 0:10 were prepared. The mean diameters of the resulting products are reported in Table 1. Myverol and SPC were used as lipophilic emulsifiers of nanoparticles in different systems (M1–M5 and S1–S5, respectively). The results showed that ratio of Precirol/squalene was a critical parameter governing the particle size. The mean size of all formulations was between 180 and 290 nm, and the polydispersity was <0.25. When increasing the squalene percentage in the lipid matrix from 0% to 80% (M1–M4 and S1–S4), the mean particle size decreased. The size again increased when the squalene percentage reached 100% (LEs, M5, and S5). There were no large discrepancies between the mean diameters of the Myverol and SPC systems. After loading lovastatin within the developed nanoparticles, the size significantly increased ($p < 0.05$) except in the SPC system with pure Precirol (S1) as shown in Table 1. Polydispersity with lovastatin loading remained at <0.25, except for the SPC system with pure squalene (S5), for which the polydispersity increased from 0.22 to 0.34. This suggests the instability of LEs after drug incorporation.

Table 1
The characterization of the lipid nanoparticles by particle size, zeta potential, and lovastatin encapsulation percentage.

Code	Lipophilic emulsifier	Precirol:squalene	Mean diameter (nm)	Mean diameter with drug (nm)	Zeta potential (mV)	Encapsulation (%)
M1	Myverol	10:0	286.5 ± 3.7	320.1 ± 3.9	−16.5 ± 0.3	72.8 ± 2.1
M2	Myverol	8:2	276.4 ± 17.8	335.9 ± 2.3	−30.3 ± 1.0	87.6 ± 2.8
M3	Myverol	5:5	250.9 ± 1.6	278.8 ± 0.6	−32.4 ± 0.4	83.8 ± 2.5
M4	Myverol	2:8	210.4 ± 5.6	270.7 ± 8.1	−31.2 ± 1.6	79.3 ± 2.7
M5	Myverol	0:10	246.9 ± 2.9	282.1 ± 4.8	−2.7 ± 0.5	81.4 ± 9.2
S1	SPC[a]	10:0	292.6 ± 3.0	295.5 ± 4.5	−25.1 ± 1.7	64.6 ± 7.7
S2	SPC	8:2	256.7 ± 5.4	312.0 ± 3.7	−20.5 ± 1.5	76.4 ± 2.5
S3	SPC	5:5	220.8 ± 7.3	245.1 ± 0.7	−23.7 ± 0.6	71.4 ± 2.7
S4	SPC	2:8	183.2 ± 0.5	331.2 ± 16.4	−34.5 ± 0.9	68.2 ± 4.8
S5	SPC	0:10	262.5 ± 3.6	306.6 ± 5.2	−11.4 ± 0.3	73.5 ± 5.3

Each value represents the mean ± SD ($n = 3$).
[a] SPC, soybean phosphatidylcholine.

Results of the zeta potential measurements are reported in Table 1. The surface charge of the different samples was consistently negative. There was no linear correlation between the zeta potential and Precirol/squalene ratios. It was noted that LEs (M5 and S5) showed lower surface charges ($p < 0.05$) compared to formulations with Precirol (SLNs and NLCs). No significant effect of the lipid core of SLNs and NLCs on the zeta potential was observed. The incorporation of lovastatin into the lipid nanoparticles had no influence ($p > 0.05$) on the zeta potential of any of the carriers (data not shown).

3.2. Drug encapsulation efficiency

An important issue with respect to the use of lipid nanoparticles as drug carriers is their capacity for drug loading. As summarized in Table 1, lovastatin demonstrated encapsulation percentages of 73% and 65% in SLNs with Myverol (M1) and SPC (S1), respectively. The incorporation of squalene (NLCs and LEs) resulted in higher trapping efficiencies ($p < 0.05$) compared to formulations with pure Precirol. The encapsulation percentages of NLCs and LEs (M2–M5 or S2–S5) were comparable to each other ($p > 0.05$). It was observed that the Myverol system showed greater entrapment than the SPC system ($p < 0.05$) when compared at the same Precirol/squalene ratios.

3.3. Molecular environment of the lipid nanoparticles

Nile red is a dye with absorption bands which vary in shape, position, and intensity with the nature of the nanoparticulate environment. Nile red is very soluble in a lipophilic environment and shows strong fluorescence. The emission spectra of Nile red in the Myverol system with varying ratios of Precirol/squalene are depicted in Fig. 1. Decreasing the Precirol percentage reduced emissions of Nile red at 580 nm, corresponding to an increase in environmental polarity. The formulations with no or little Precirol (M4 and M5) also exhibited a spectral shift to longer wavelengths.

3.4. Partitioning of the drug between lipids and water

The partition coefficients of lovastatin between the lipids and water are given in Table 2. All log *P* values were >3, indicating extensive partitioning of lovastatin into the lipid phase. Log *P* values obtained from pure Precirol/water and squalene/water were 3.44 and 3.63, respectively. A higher partition coefficient was generally observed with the lipid phase containing higher squalene contents ($p < 0.05$), although the lipid phases of 80% and 100% Precirol showed approximately equal values.

Table 2
The partition coefficient (log *P*) between Lipids (Precirol and squalene) and water of lovastatin.

Precirol:squalene	Log *P*
10:0	3.44 ± 0.01
8:2	3.42 ± 0.01
5:5	3.48 ± 0.01
2:8	3.57 ± 0.03
0:10	3.63 ± 0.02

Each value represents the mean ± SD ($n = 5$).

3.5. In vitro release kinetics of the drug from lipid nanoparticles

In order to develop a prolonged release system with general applicability, it is of great importance to understand the release mechanism and kinetics. The levels of in vitro lovastatin release from nanoparticles of different compositions are shown in Fig. 2. The amount of lovastatin released from each system was plotted as a function of time. Because of the low solubility of lovastatin in water, a mixture of propylene glycol/ethanol (9:1) was selected as the control group. The free control showed quick release of lovastatin, with a cumulative 43% released at 24 h. The inclusion of the drug into lipid nanoparticles significantly reduced ($p < 0.05$) the release. Release percentages from the Myverol system varied from 3% to 17% at 24 h depending upon differences in the Precirol/squalene ratios (Fig. 4A). Pure Precirol (M1) exhibited the smallest release, followed by pure squalene (M5), 80% Precirol (M2), 50% Precirol (M3), and 20% Precirol (M4).

Fig. 2B shows the release-time profiles of lovastatin from the SPC system. The trend of release from lipid nanoparticles with SPC greatly differed from that of the Myverol system. SLNs and NLCs (S1–S4) revealed an approximately equal drug release without statistical significance ($p > 0.05$). LEs (S5) provided more-rapid drug delivery compared to SLNs and NLCs. The SPC system exhibited slower release than the corresponding Myverol system.

3.6. In vivo pharmacokinetics

Fig. 3A shows the concentration–time profiles of lovastatin in circulation after intravenous injection. Lovastatin was rapidly degraded after injection. Almost no drug concentration was detected at 4 h after administration. The $AUC_{0\to\infty}$ of the intravenous lovastatin was 1770.53 ± 386.84 μg h/ml. Fig. 3B illustrates the concentration versus time profiles of lovastatin with the administration of a single oral dose to three groups, including the free control and NLCs with a Precirol/squalene ratio of 5:5 (M3 and S3). Animals receiving lovastatin gavage exhibited a concentration–time profile

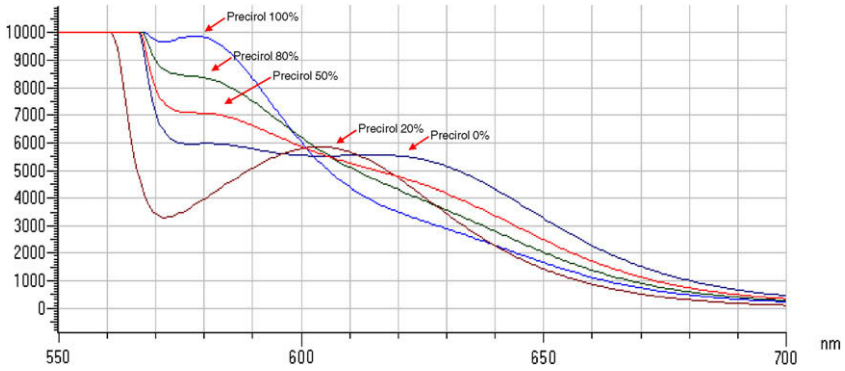

Fig. 1. Fluorescence emission spectra of Nile red (1 ppm) in lipid nanoparticle systems with different Precirol percentages of 0–100%. (For interpretation of the references to colour in this figure legend, the reader is referred to the web version of this article.)

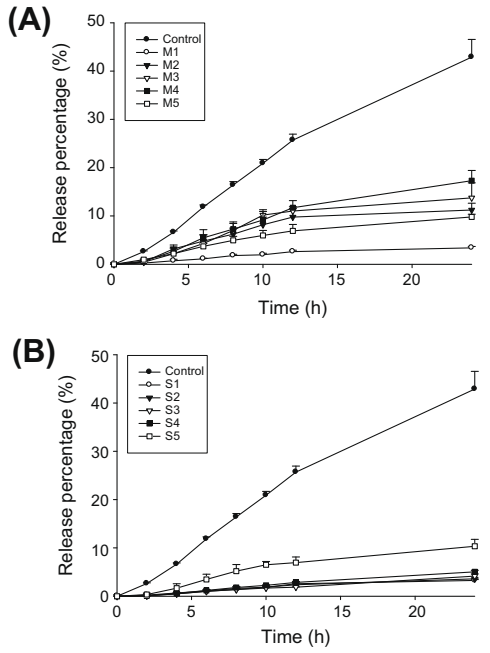

Fig. 2. In vitro release percentage (%)-time profiles of lovastatin (1% w/v) across a cellulose membrane from lipid nanoparticulate systems containing Myverol (A) or soybean phosphatidyl choline (SPC) (B) as the lipophilic emulsifier. Each value represents the mean and SD ($n = 4$).

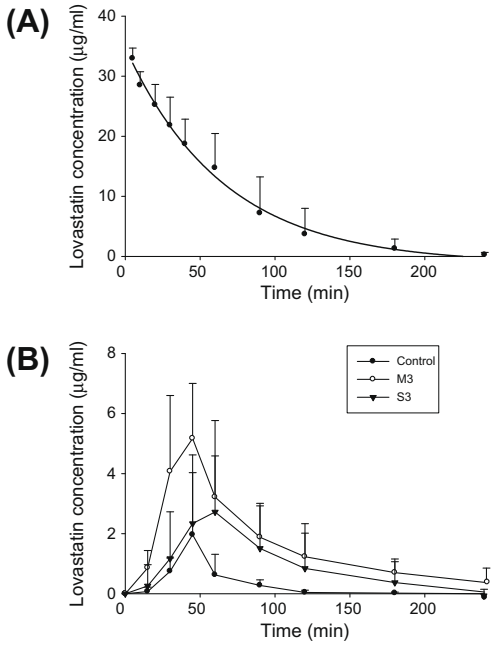

Fig. 3. Mean plasma concentration of lovastatin–time curves after oral administration of lovastatin to rats at a dose of 100 mg/kg from a control solution and nanostructured lipid carriers (NLCs). Each value represents the mean and SD ($n = 9$).

characterized by an early peak concentration followed by a continuous decay in the plasma concentration. This is consistent with fast and complete absorption of the bioavailable drug fraction. At all times, the mean plasma concentrations were higher in rats treated with NLCs than in those treated with the control solution. Pharmacokinetic parameters obtained by a non-compartmental analysis after the oral administration of lovastatin are listed in Table 3. Following oral ingestion of the control group, Myverol system (M3),

Table 3
Pharmacokinetic parameters of lovastatin (100 mg/kg) after oral administration of control solution and nanostructured lipid carriers (NLCs) with Myverol or SPC to rats.

Parameter	Control	NLCs with Myverol (M3)	NLCs with SPC (S3)
C_{max} (μg/ml)[a]	2.32 ± 1.69	5.88 ± 1.74	3.36 ± 2.69
T_{max} (min)[b]	37.50 ± 8.66	38.08 ± 7.48	61.50 ± 16.66
$AUC_{0\to\infty}$ (μg h/ml)[c]	66.11 ± 50.28	423.83 ± 144.18	222.81 ± 124.16
F (%)[d]	3.73 ± 2.84	23.94 ± 8.14	12.58 ± 7.01
MRT (min)[e]	53.73 ± 3.89	82.15 ± 19.15	73.22 ± 19.25
$t_{1/2}$ (min)[f]	32.00 ± 9.92	84.68 ± 46.32	32.54 ± 14.12
V_z/F (l) [g]	93.46 ± 35.40	30.71 ± 18.51	44.25 ± 27.46

Each value represents the mean ± SD ($n = 9$).
[a] C_{max}, maximum plasma concentration.
[b] T_{max}, time to reach C_{max}.
[c] $AUC_{0\to\infty}$, area under the plasma concentration–time curve.
[d] F, absolute bioavailability.
[e] MRT, mean residence time.
[f] $t_{1/2}$, elimination half-life.
[g] V_z/F, apparent volume of distribution.

and SPC system (S3), the average peak plasma concentrations (C_{max}) were 2.32, 5.88, and 3.36 μg/ml at 37.50, 38.08, and 61.50 min, respectively. The $AUC_{0\to\infty}$ value of lovastatin after oral gavage of the Myverol system was respectively 6.4- and 3.4-fold higher than those obtained with the free control and SPC system. It is clear that a significantly higher ($p < 0.05$) bioavailability (F) was found when administered as the Myverol system compared to the SPC system and the control. The MRT was significantly longer ($p < 0.05$) for NLCs with Myverol, followed by the SPC system and free control. The Myverol system showed the highest elimination $t_{1/2}$ of 84.68 min. The $t_{1/2}$ values of the SPC system and control solution were roughly equivalent ($p > 0.05$).

3.7. In vivo bioluminescence imaging

The residence of nanoparticles in the GI tract was evaluated by bioluminescence imaging following the oral delivery of sulforhodamine B-labeled NLCs. Because of a low intrinsic bioluminescence in mammalian tissues, a high signal-to-noise ratio can be achieved with in vivo optical imaging. Fig. 4 shows bioluminescence images of representative animals treated with the control solution, Myverol system (M3), and SPC system (S3) (left to right). Fluorescence

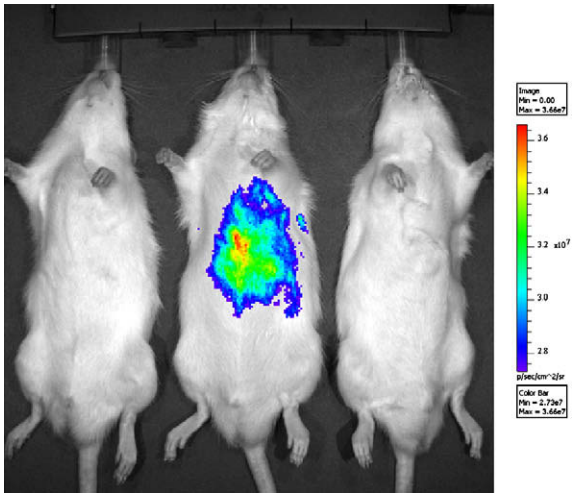

Fig. 4. Bioluminescence imaging of representative animals at 10 min following oral administration of sulforhodamine B in a control solution, nanostructured lipid carriers (NLCs) with Myverol, and NLCs with soybean phosphatidyl choline (SPC) (left to right). (For interpretation of the references to colour in this figure legend, the reader is referred to the web version of this article.)

signals in the abdominal region were evident after deducting the auto-fluorescence of the animal itself. Immediately following administration for 10 min, the signal was clearly visualized in the abdominal region of Myverol system-treated rats. However, no signal was detected in groups treated with the solution and SPC system. This indicates that a higher accumulation of sulforhodamine B was observed following the administration of NLCs with Myverol than the free form or NLCs with SPC.

4. Discussion

Poor oral bioavailability in patients and a short half-life of lovastatin therapy remain clinical issues. Lovastatin preparations with a long-acting effect are particularly desirable. The purpose of this work was to develop novel delivery systems that can be used to administer oral lovastatin for enhanced and prolonged efficacy. A further aim included modulating the physicochemical characteristics and release rate by changing the solid lipid/liquid lipid ratios of the nanoparticles. The experimental results showed that lovastatin loading in NLCs offered benefits in terms of increased oral absorption and sustained drug release. The selection of optimal emulsifiers is important to facilitate these advantages.

It is known that using two emulsifiers, with respective hydrophilic and lipophilic natures, yields better stabilization of the dispersive system [13]. The results showed that lovastatin nanoparticulate dispersions were obtained with quite-different stabilizer systems. Pure Precirol (SLNs) led to a larger particle size than formulations containing squalene (NLCs and LEs). Precirol is a fatty ester with different alkyl chains. Distances between fatty acid chains can be increased by using glycerides composed of different fatty acids [14], resulting large spaces among the particles. Another possibility is the influence of viscosity since the trend for an increased particle size may be due to an increasing viscosity [15]. The addition of squalene to the inner phase may have tended to promote the formation of a small-particle population as a result of higher molecular mobility and lower viscosity [16]. However, pure squalene of 100% (LEs, M5, and S5) did not produce the smallest particle size. According to the results of the molecular environment, the polarity of nanoparticles was well controlled by the ratio of Precirol/squalene. The emulsifier system with a determined hydrophile–lipophile balance (HLB) may well have stabilized the NLCs which had a moderate polarity, resulting in a smaller size compared to SLNs and LEs. It was suggested [17] that surface-active partial glycerides such as Precirol and Compritol facilitate emulsification and form rigid interfacial films. The absence of Precirol from the nanoparticles should tend to increase the size distribution due to insufficient emulsification. The zeta potential is known to be predictive of the stability of nanoparticles [18]. LEs (M5 and S5) with lower zeta potential values compared to NLCs may be unstable, resulting in a rapid aggregation among particles. Nevertheless, this explanation is not a universal rule, since SLNs (M1 and S1) with the largest size had moderate surface charges.

PF68 is a non-ionic species. The negative charge shown by nanoparticles is believed to have resulted from the presence of lipophilic emulsifiers. Some free fatty acids derived from the hydrolysis of monoglycerides in Myverol (palmitic acid monoglycerides) may have occurred [19]. Anionic fractions such as phosphatidylserine, phosphatidic acid, phosphatidylglycerol, and phosphatidylinositol in SPC with 80% phosphatidylcholine are responsible for the negative surface charges of the SPC system [20]. Formulations with Precirol (SLNs and NLCs) showed a higher negative charge compared to those without it (LEs). The glyceride structure in Precirol may liberate anionic fatty acids, the same as the phenomenon with Myverol. Hence Precirol contributed to the negative charge of SLN and NLC interfaces. Pure squalene, on the other hand, is a non-ionic species. However, it should be mentioned that greater amounts of Precirol did not produce higher negative charges. The incorporation of lovastatin in systems did not affect values of the zeta potential. This indicates that most of the lovastatin molecules resided in the lipid core, not in the nanoparticle shell.

Carriers of NLCs and LEs, but not of SLNs, promoted the lovastatin encapsulation yield. Colloidal dispersions made of mixtures of solid and liquid lipids were described as overcoming the poor drug-loading capacity of SLNs [5,14]. Precirol forms highly crystalline particles with a perfect lattice which leads to drug expulsion. The incorporation of a liquid and solid lipid can lead to massive crystal order disturbances, and the matrix shows great imperfections in the crystal lattice creating sufficient space to accommodate drug molecules [15,21]. Our previous study [19] demonstrated the fact that SLNs produced an inner phase which was crystalline. As examined by differential scanning calorimetry (DSC), the inner phase of NLCs was solid not crystalline. The partitioning nature of lovastatin between the lipid and aqueous phases can provide clues about its entrapment in the nanoparticles. The log P results indicated that an increase in the amount of squalene increased lovastatin partitioning in the lipid phase. This is reasonable since the solubility of drugs is basically higher in liquid than solid lipids [14].

The replacement of Myverol by SPC contributed to a reduction in lovastatin encapsulation. It was assumed that the amphiphilic nature of the emulsifier would facilitate the orientation of the lipid part towards the lipid core and the hydrophilic group towards the external aqueous phase. The crystallization tendency of the inner core decreased with the addition to the interface of phospholipids, which possess two hydrophobic chains in the structures [22]. Moreover, the presence of phospholipids at the interface containing PF68 caused a rearrangement of the monolayer membrane to a disordered form [23]. Some free fatty acids can be derived from Myverol according to the negative zeta potential of the Myverol system. Alkali fatty acids are thought to yield mixed films with a higher packing density of interfacial film-forming components [24,25]. The tight structure of this membrane may prevent the loss of lovastatin across the interface during emulsification.

The polarity (molecular environment) of lipid nanoparticles can be investigated by the fluorescence emission of Nile red. The intensity of Nile red is quenched in more-hydrophilic environments [26]. The high polarity also leads to a spectral shift to longer wavelengths. The results showed that the polarity of nanoparticles generally decreased following an increase in Precirol contents, indicating the lipophilic character of Precirol. Crystallization of the solid lipid reduced the accommodation capacity for foreign molecules and caused considerable expulsion and aggregation of Nile red, thus reducing the fluorescence intensity [27]. However, that was not the case in the present study. This indicates the limited role of expulsion with Precirol. This inference was confirmed by the encapsulation efficiency, since the discrepancy in the amount of lovastatin entrapment between the systems with pure Precirol (SLNs) and squalene (NLCs and LEs) was finite, although SLNs showed a lower drug-loading capacity.

The amount of lovastatin released from the free control was limited, with ~40% of the drug being released over 24 h. This may have been due to the use of the Franz cell assembly. Since a drug is released to a definitive space in the receptor (5.5 ml) and diffusion area (0.785 cm^2), drug loading in the receptor compartment is limited. There might be only a small concentration gradient between the donor and receptor compartments. Nevertheless, this setup is still useful for differentiating the relative release capabilities of various formulations [28,29]. The slower release of lovastatin from nanoparticles suggests that lovastatin was homogeneously dispersed in the lipid matrix. The drug is stably retained in the lipid core for a determined duration, followed by its

slow release into the external phase. The sustained release of an incorporated drug in a delivery system is an important characteristic quite often correlated with improved pharmacokinetics and efficacy.

The results of lovastatin release suggest that it is possible to modify the release profiles as a function of the lipid matrix and emulsifier type. As observed with the Myverol system, the formulation with 100% Precirol (SLNs, M1) exhibited the slowest release of lovastatin. Precirol has a crystalline state. Therefore, the mobility of the incorporated drug was reduced due to decreased diffusion out of the inner phase [22]. Precirol showed high lipophilicity according to the determination of polarity. Precirol may strongly interact with the lipophilic lovastatin, thus retarding the release capability. Another possibility is that the viscosity is related to the strength of the interfacial film [19,30]. The release of lovastatin increased following an increase in the squalene percentage to 80%. The liquid oil is soft and possesses considerably higher solubility for lipophilic drugs [15], in which the drugs can be easily released by drug diffusion and matrix erosion. However, 100% squalene (LEs, M5) in the lipid core did not produce the highest release. Lovastatin released from LEs of the Myverol system was lower than that from NLCs. The factor contributing to the retarded release rate of LEs may have been the smaller surface area due to the larger particle size. A decrease in release would therefore be expected because of the insufficient total surface area to release the drug [22,31]. This hypothesis can also explain the slowest drug release of SLNs, which had the largest size. The release results suggest that controlled adjustment of release can be achieved by modifying the nature of the lipid matrix. No linear relation between the Precirol/squalene ratios and lovastatin release was observed. Thus, each ratio leads to a distinguishable lipid-based formulation. The inner phases of SLNs, NLCs, and LEs may present a state of an ordered crystal, imperfect solid, and liquid, respectively.

SPC was shown to exert a quite different release behavior compared to nanoparticles with Myverol. The mechanisms predominating lovastatin delivery should differ in the Myverol and SPC systems. The replacement of Myverol by SPC further retarded lovastatin release. The release profiles from SLNs and NLCs containing SPC were approximately the same. This indicates that the interfacial membrane with SPC might act as a rate-limiting barrier. The effect of release modulation by the inner phase of the Myverol system was diminished by SPC replacement. The phenomenon seems to be correlated with specific interactions between phospholipids and the solid lipid matrix. A strong binding of phospholipids to the solid triglyceride matrix may have occurred to immobilize the interfacial film [32,33]. This immobilization allowed the retarded release of lovastatin across the SPC barrier. This effect was not observed for LEs, since this carrier exhibited greater drug release. This may have been because phospholipids are preferentially adsorbed by the triglyceride nanocrystals rather than by the emulsion droplets [32].

In general, a higher load of the drug into nanoparticles allows a slower and more prolonged release. However, this was not the case in this study since the SPC system showed lower lovastatin encapsulation and slower drug release compared to the Myverol system. Although Myverol provided a rigid interfacial structure as indicated by the encapsulation profiles, it is possible that glycerides undergo degradation to fatty acids during incubation, which can compete with formulation emulsifiers for positioning on the interface. Fatty acids can form mixed micelles that might enhance the partitioning of the drug out of the lipid nanoparticles [34]. Lovastatin can easily escape from the nanoparticles during the in vitro release period. This phenomenon was not detected in the carriers with SPC, which demonstrates that lovastatin was stably and restrictedly retained in the SPC system for a longer time, once the drug was already included in the inner matrix. Further work is needed to elucidate the mechanisms.

The oral bioavailability of lovastatin from the control solution was 3.73% and highly variable. The results were similar to those in a human study [35], which showed a bioavailability of ~5%. After oral administration of NLCs to rats, the bioavailability of lovastatin increased considerably, especially with the system containing Myverol (M3). The variability of bioavailability values was smaller with NLCs than with the free control, indicating less inter-subject variation using nanoparticles. Since lovastatin was completely dissolved in the control solution, enhancement of the solubility and dissolution rate could be ruled out for explaining the higher oral absorption of NLCs. The ability of the lipid nanoparticles to enhance the transport of the drugs across the GI tract was attributed to different mechanisms including: (i) lymphatic transport, (ii) mucoadhesion, (iii) sustained drug release, and (v) drug protection efficiency [36,37].

Lovastatin is considered to be a reasonable substrate for intestinal lymphatic transport [34]. The inclusion of lipophilic drugs into lipid nanoparticles can enhance targeting to the lymph system [38]. Nanoparticles are composed of a lipid core that can stimulate chylomicron formation, which ultimately carries the carrier along with the drug by following the classical transcellular mechanism of lipid absorption [39]. The efficiency is directly correlated with the specific surface area of the particles. Compared to a simple lipid vehicle, incorporation of the drug in the lipid phase of NLCs increased the lipid surface area and subsequently the bioavailability. Another mechanism is that nanoparticles in general possess adhesive properties. The absorption-enhancing effect of orally administered nanoparticles was attributed to the adhesion of the particles to the gut wall [11]. The adhesion of lipid nanoparticles to the mucus can improve the residence time and contact of the drug with the underlying epithelium, thus increasing the concentration gradient [37]. Another observation is a decrease in V_z/F after the incorporation of lovastatin into nanoparticles. This means a reduction of the distribution to peripheral tissues. It is beneficial for lovastatin to lower cholesterol in circulation system. It may also infer the possible permeation of intact nanoparticles across GI membrane. Further works are necessary to explore this possibility.

A previous study [40] suggested increased oral bioavailability and prolonged efficacy with a lovastatin extended-release tablet. The release of lovastatin from the tablet was controlled by osmotic pressure. This allows the release of the drug at a constant and controlled rate. Our release experiment indicated a controlled manner of lovastatin release from NLCs at a determined rate. Hence, the enhanced efficacy of NLCs may have been the result of continuous and more sustained delivery of lovastatin to the circulation. This could be confirmed by the longer MRT of NLCs compared to the control solution. Lovastatin is largely metabolized in the GI tract to its major metabolites, and the generated metabolic pattern is similar to that in the liver [9,34]. Lovastatin should be protected from the harsh gastric and intestinal environments. The advantage of nanoparticles over a solution is the protection of the drug by the lipids from chemicals and enzymatic degradation, thereby delaying in vivo metabolism [41,42]. The same effect was observed in a study of Ge et al. [43], which utilized a dry emulsion to protect lovastatin against intestinal metabolism and improved the bioavailability.

Although NLCs can improve the oral absorption of lovastatin, there was a difference in the pharmacokinetics between the NLCs containing Myverol and SPC. The bioavailability and half-life in rats treated with the Myverol system were ~2-fold higher than those treated with the SPC system. In order to explore the effect of the lipophilic emulsifier on oral lovastatin delivery, in vivo bioluminescence imaging was examined. Bioluminescence imaging is a noninvasive and real-time technique for performing an in vivo diagnostic

Table 4
The particle size of nanostructured lipid carriers (NLCs) with Myverol or SPC after incubation in double-distilled water and 0.1 N hydrochloric acid solution at 5 min and 60 min.

Formulation	Double-distilled water		0.1 N HCl solution	
	5 min	60 min	5 min	60 min
NLCs with Myverol (M3)	275.1 ± 1.4	298.5 ± 0.4	644.6 ± 19.8	1313.5 ± 413.0
NLCs with SPC (S3)	269.5 ± 1.0	331.3 ± 5.0	2413.8 ± 81.0	4844.8 ± 452.4

Each value represents the mean ± SD ($n = 3$).

study on animal subjects. It is a high-throughput and sensitive imaging modality [44]. The excitation and emission wavelengths used in this study to detect abdominal accumulation were >600 nm. Longer wavelengths of bioluminescence in the red and near-infrared regions of the spectrum are transmitted through mammalian tissues more efficiently than are shorter wavelengths of light [45]. A significant fluorescence signal was observed in the abdominal region of rats treated with NLCs containing Myverol (M3). It was surprising that there was no signal detected in the abdominal region with the SPC system (S3). This suggests poor stability and retention of the SPC system in the GI tract. To understand the behavior of NLCs in the GI tract, the size stability of Myverol and SPC systems was determined in ddH_2O and a 0.1 N HCl solution at a 1:100 dilution. As shown in Table 4, both systems exhibited instantaneous and massive aggregation following incubation in ddH_2O and an HCl solution for 5 and 60 min. A significantly greater aggregation ($p < 0.05$) was observed in the HCl solution compared to ddH_2O. The size of the SPC system increased from 221 to 2414 nm after only a 5-min incubation. At the same time, the Myverol system increased from 251 to 645 nm. A progressive increase in particle size was observed from 5 to 60 min. The results indicate significant instability of NLCs with SPC in the gastric environment.

The microclimate of the stomach favors particle aggregation due to its acidity and high ionic strength [1]. Particle aggregation can result in breakdown of the lipid formulations. Müller et al. [11] revealed that the emulsifier layer controls the anchoring of the lipase/co-lipase complex. In the case of phospholipids as a stabilizer, the anchoring of the complex leads to rapid degradation. This can result in lower bioavailability and bioluminescence intensity of the SPC system compared to the Myverol system. However, oral absorption with the SPC system was still greater than that of the free solution. This can be attributed to the steric hindrance of the anchoring by PF68 [11,46], which is a hydrophilic emulsifier used in this study. Carriers with Myverol were able to protect the drug and produced sustained release of the drug. This is beneficial with lovastatin since the extended release effect can produce significantly greater cholesterol reduction than an equal dose of lovastatin of the immediate-release form [6]. These results also indicated that the composition of NLCs can affect the physicochemical characteristics and also the behaviors of oral absorption. A well-defined study protocol is further required to elucidate the mechanisms of oral lovastatin delivery by NLCs.

5. Conclusions

The purpose of this study was to assess the feasibility of using NLCs to promote the oral absorption of lovastatin. The physicochemical properties and release rate showed that each nanoparticulate system (SLNs, NLCs, or LEs) had distinguishable characteristics. The controlled adjustment of drug release was achieved by modifying the lipid matrix with various Precirol/squalene ratios. The results exhibited that the lipophilic emulsifiers influenced the drug release and the stability of NLCs, which affected the in vivo performance of the nanoparticles. An oral pharmacokinetic study was conducted in rats, and the results showed that NLCs produced a significant improvement in the bioavailability compared to the free solution. The types of emulsifier had an important influence on the oral absorption of lovastatin, and NLCs with Myverol were found to be more stable in the gastric environment compared to those with SPC. Lovastatin administration from Myverol-containing NLCs led to plasma concentrations which were greater, less variable, and more prolonged than when the drug was given in the free form. The changes in pharmacokinetic parameters with NLCs can improve the clinical efficacy of lovastatin.

References

[1] K.K. Sawant, S.S. Dodiya, Recent advances and patents on solid lipid nanoparticles, Recent Pat. Drug Deliv. Formulat. 2 (2008) 120–135.
[2] R.H. Müller, K. Mäder, S. Gohla, Solid lipid nanoparticles (SLN) for controlled drug delivery – a review of the state of the art, Eur. J. Pharm. Biopharm. 50 (2000) 161–177.
[3] H. Yuan, L.L. Wang, Y.Z. Du, J. You, F.Q. Hu, S. Zeng, Preparation and characteristics of nanostructured lipid carriers for control-releasing progesterone by melt-emulsification, Colloids Surf. B – Biointerf. 60 (2007) 174–179.
[4] V. Teeranachaideekul, R.H. Müller, V.B. Junyaprasert, Encapsulation of ascorbyl palmitate in nanostructured lipid carriers (NLC): effects of formulation parameters on physicochemical stability, Int. J. Pharm. 340 (2007) 198–206.
[5] R.H. Müller, R.D. Petersen, A. Hommoss, J. Pardeike, Nanostructured lipid carriers (NLC) in cosmetic dermal products, Adv. Drug Deliv. Rev. 59 (2007) 522–530.
[6] M.H. Davidson, P. Lukacsko, J.X. Sun, G. Phillips, E. Walters, A. Sterman, R. Niecestro, L. Friedhoff, A multiple-dose pharmacodynamic, safety, and pharmacokinetic comparison of extended- and immediate-release formulations of lovastatin, Clin. Ther. 24 (2002) 112–125.
[7] G.E. Gutierrez, D. Lalka, I.R. Garrett, G. Rossini, G.R. Mundy, Transdermal application of lovastatin to rats causes profound increases in bone formation and plasma concentrations, Osteoporos. Int. 17 (2006) 1033–1042.
[8] T. Martín-Jiménez, M. Lindeblad, I.M. Kapetanovic, Y. Chen, A. Lyubimov, Comparing pharmacokinetic and pharmacodynamic profiles in female rats orally exposed to lovastatin by gavage versus diet, Chem. Biol. Interact. 171 (2008) 142–151.
[9] W. Jacobsen, G. Kirchner, K. Hallensleben, L. Mancinelli, M. Deters, I. Hackbarth, K. Baner, L.Z. Benet, K. Sewing, U. Christians, Small intestinal metabolism of the 3-hydroxy-3-methylglutaryl-coenzyme A reductase inhibitor lovastatin and comparison with pravastatin, J. Pharmacol. Exp. Ther. 291 (1999) 131–139.
[10] L. Reyderman, T. Kosoglou, T. Boutros, M. Seiberling, P. Statkevich, Pharmacokinetic interaction between ezetimibe and lovastatin in healthy volunteers, Curr. Med. Res. Opin. 20 (2004) 1493–1500.
[11] R.H. Müller, S. Runge, V. Ravelli, A.F. Thünemann, E.B. Souto, Oral bioavailability of cyclosporine: solid lipid nanoparticles (SLN®) versus drug nanocrystals, Int. J. Pharm. 317 (2006) 82–89.
[12] S.C. Wang, L.K. Ho, J.C. Yen, T.H. Tsai, An automated blood sampling system to measure lovastatin level in plasma and feces, Biomed. Chromatogr. 20 (2006) 911–916.
[13] M.A. Casadei, F. Cerreto, S. Cesa, M. Giannuzzo, M. Feeney, C. Marianecci, P. Paolicelli, Solid lipid nanoparticles incorporated in dextran hydrogels: a new drug delivery system for oral formulations, Int. J. Pharm. 325 (2006) 140–146.
[14] R.H. Müller, M. Radtake, S.A. Wissing, Nanostructured lipid matrices for improved microencapsulation of drugs, Int. J. Pharm. 242 (2002) 121–128.
[15] F.Q. Hu, S.P. Jiang, Y.Z. Du, H. Yuan, Y.Q. Ye, S. Zeng, Preparation and characteristics of monostearin nanostructured lipid carriers, Int. J. Pharm. 314 (2006) 83–89.
[16] J.J. Wang, K.S. Liu, K.C. Sung, C.Y. Tsai, J.Y. Fang, Lipid nanoparticles with different oil/fatty ester ratios as carriers of buprenorphine and its prodrugs for injection, Eur. J. Pharm. Sci. 38 (2009) 138–146.
[17] V. Jenning, A.F. Thünemann, S.H. Gohla, Characterization of a novel solid lipid nanoparticle carrier system based on binary mixtures of liquid and solid lipids, Int. J. Pharm. 199 (2000) 167–177.
[18] S. Poullain-Termeau, S. Crauste-Manciet, D. Brossard, S. Muhamed, G. Nicolaos, R. Farinotti, C. Barthélémy, H. Robert, P. Odou, Effect of oil-in-water submicron emulsion surface charge on oral absorption of a poorly water-soluble drug in rats, Drug Deliv. 15 (2008) 503–514.
[19] J.Y. Fang, C.L. Fang, C.H. Liu, Y.H. Su, Lipid nanoparticles as vehicles for topical psoralen delivery: solid lipid nanoparticles (SLN) versus nanostructured lipid carriers (NLC), Eur. J. Pharm. Biopharm. 70 (2008) 633–640.
[20] C.F. Hung, C.L. Fang, M.H. Liao, J.Y. Fang, The effect of oil components on the physicochemical properties and drug delivery of emulsions: tocol emulsion versus lipid emulsion, Int. J. Pharm. 335 (2007) 193–202.

[21] E.B. Souto, S.A. Wissing, C.M. Barbosa, R.H. Müller, Development of a controlled release formulation based on SLN and NLC for topical clotrimazole delivery, Int. J. Pharm. 278 (2004) 71–77.
[22] A. zur Mühlen, C. Schwarz, W. Mehnert, Solid lipid nanoparticles (SLN) for controlled drug delivery – drug release and release mechanism, Eur. J. Pharm. Biopharm. 45 (1998) 149–155.
[23] J.Y. Fang, C.F. Hung, M.H. Liao, C.C. Chien, A study of the formulation design of acoustically active lipospheres as carriers for drug delivery, Eur. J. Pharm. Biopharm. 67 (2007) 67–75.
[24] K. Buszello, S. Harnisch, R.H. Müller, B.W. Müller, The influence of alkali fatty acids on the properties and the stability of parenteral o/w emulsions modified with Solutol HS15®, Eur. J. Pharm. Biopharm. 49 (2000) 143–149.
[25] J.J. Wang, K.C. Sung, O.Y.P. Hu, C.H. Yeh, J.Y. Fang, Submicron lipid emulsion as a drug delivery system for nalbuphine and its prodrugs, J. Control. Release 115 (2006) 140–149.
[26] S. Lombardi Borgia, M. Regehly, R. Sivaramakrishnan, W. Mehnert, H.C. Korting, K. Danker, B. Röder, K.D. Kramer, M. Schäfer-Korting, Lipid nanoparticles for skin penetration enhancement: correlation to drug localization within the particle matrix as determined by fluorescence and parelectric spectroscopy, J. Control. Release 110 (2005) 151–163.
[27] K. Jores, A. Haberland, S. Wartewig, K. Mäder, W. Mehnert, Solid lipid nanoparticles (SLN) and oil-loaded SLN studied by spectrofluorometry and Raman spectroscopy, Pharm. Res. 22 (2005) 1887–1897.
[28] P.P. Constandinides, K.J. Lambert, A.K. Tustian, B. Schneider, S. Lalji, W. Ma, B. Wentzel, D. Kessler, D. Worah, S.C. Quay, Formulation development and antitumor activity of a filter-sterilizable emulsion of paclitaxel, Pharm. Res. 17 (2000) 175–182.
[29] T.L. Hwang, Y.K. Lin, C.H. Chi, T.H. Huang, J.Y. Fang, Development and evaluation of perfluorocarbon nanobubbles for apomorphine delivery, J. Pharm. Sci. 98 (2009) 3735–3747.
[30] T.G. Mason, New fundamental concepts in emulsion rheology, Curr. Opin. Colloid Interf. Sci. 4 (1999) 231–238.
[31] X. Zhang, W. Pan, L. Gan, C. Zhu, Y. Gan, S. Nie, Preparation of a dispersible PEGylate nanostructured lipid carriers (NLC) loaded with 10-hydroxycamptothecin by spray-drying, Chem. Pharm. Bull. 56 (2008) 1645–1650.
[32] H. Bunjes, M.H.J. Koch, K. Westesen, Influence of emulsifiers on the crystallization of solid lipid nanoparticles, J. Pharm. Sci. 92 (2003) 1509–1520.
[33] M.A. Schubert, M. Harms, C.C. Müller-Goymann, Structural investigations on lipid nanoparticles containing high amounts of lecithin, Eur. J. Pharm. Sci. 27 (2006) 226–236.
[34] G. Suresh, K. Manjunath, V. Venkateswarlu, V. Satyanarayana, Preparation, characterization, and in vitro and in vivo evaluation of lovastatin solid lipid nanoparticles, AAPS PharmSciTech 8 (2007) (Article 24).
[35] P.J. Neuvonen, J.T. Backman, M. Niemi, Pharmacokinetic comparison of the potential over-the-counter statins simvastatin, lovastatin, fluvastatin and pravastatin, Clin. Pharmacokinet. 47 (2008) 463–474.
[36] S. Yang, J. Zhu, Y. Lu, B. Liang, C. Yang, Body distribution of camptothecin solid lipid nanoparticles after oral administration, Pharm. Res. 16 (1999) 751–757.
[37] M. Garcia-Fuentes, C. Prego, D. Torres, M.J. Alonso, A comparative study of the potential of solid triglyceride nanostructures coated with chitosan or poly(ethylene glycol) as carriers for oral calcitonin delivery, Eur. J. Pharm. Sci. 25 (2005) 133–143.
[38] L. Priano, D. Esposti, R. Esposti, G. Castagna, L. De Medici, F. Fraschini, M.R. Gasco, A. Mauro, Solid lipid nanoparticles incorporating melatonin as new model for sustained oral and transdermal delivery systems, J. Nanosci. Nanotechnol. 7 (2007) 3596–3601.
[39] R. Paliwal, S. Rai, B. Vaidya, K. Khatri, A.K. Goyal, N. Mishra, A. Mehta, S.P. Vyas, Effect of lipid core material on characteristics of solid lipid nanoparticles designed for oral lymphatic delivery, Nanomedicine 5 (2009) 184–191.
[40] M.P. Curran, K.L. Goa, Lovastatin extended release. A review of its use in the management of hypercholesterolaemia, Drugs 63 (2003) 685–699.
[41] Y.F. Luo, D.W. Chen, L.X. Ren, X.L. Zhao, J. Qin, Solid lipid nanoparticles for enhancing vinpocetine's oral bioavailability, J. Control. Release 114 (2006) 53–59.
[42] P.D. Marcato, N. Durán, New aspects of nanopharmaceutical delivery systems, J. Nanosci. Nanotechnol. 8 (2008) 2216–2229.
[43] Z. Ge, X.X. Zhang, L. Gan, Y. Gan, Redispersible, dry emulsion of lovastatin protects against intestinal metabolism and improves bioavailability, Acta Pharmacol. Sinica 29 (2008) 990–997.
[44] C. Kuo, O. Coquoz, T.L. Troy, H. Xu, B.W. Rice, Three-dimensional reconstruction of in vivo bioluminescent sources based on multispectral imaging, J. Biomed. Opt. 12 (2007) 024007.
[45] R.S. Negrin, C.H. Contag, In vivo imaging using bioluminescence: a tool for probing graft-versus-host disease, Nat. Rev. Immunol. 6 (2006) 484–490.
[46] N. Zhang, Q. Ping, G. Huang, W. Xu, Y. Cheng, X. Han, Lectin-modified solid lipid nanoparticles as carriers for oral administration of insulin, Int. J. Pharm. 327 (2006) 153–159.